Synchronization and plateau splitting of coupled oscillators with long-range power-law interactions

Huan-Yu Kuo and Kuo-An Wu*
Department of Physics, National Tsing-Hua University, 30013 Hsinchu, Taiwan
(Received 4 September 2015; published 21 December 2015)

We investigate synchronization and plateau splitting of coupled oscillators on a one-dimensional lattice with long-range interactions that decay over distance as a power law. We show that in the thermodynamic limit the dynamics of systems of coupled oscillators with power-law exponent $\alpha \leqslant 1$ is identical to that of the all-to-all coupling case. For $\alpha > 1$, oscillatory behavior of the phase coherence appears as a result of single plateau splitting into multiple plateaus. A coarse-graining method is used to investigate the onset of plateau splitting. We analyze a simple oscillatory state formed by two plateaus in detail and propose a systematic approach to predict the onset of plateau splitting. The prediction of breaking points of plateau splitting is in quantitatively good agreement with numerical simulations.

DOI: 10.1103/PhysRevE.92.062918 PACS number(s): 05.45.−a, 82.40.Ck, 89.75.Fb, 89.75.Kd

I. INTRODUCTION

Synchronization is the phenomenon where two or more distinct individuals come to behave in unison due to interactions. The synchronization phenomena are commonly seen in a wide range of physical, chemical, and biological systems, such as oscillating chemical reactions [1–3], Josephson junction arrays [4–7], audience clapping [8,9], pendulum and crowd synchrony through a common medium [10–12], fireflies flashing [13–15], human brain network, and neuronal systems [16–21].

The first mathematical model on collective synchronization dates back to the mid-1960s by Winfree [22]. He reduced the complex dynamics of coupled limit-cycle oscillators to the phase equations of oscillators under the assumptions of weakly coupled oscillators and nearly identical oscillators. Kuramoto refined Winfree's concept and recast the phase model to be mathematically tractable [2,23–25]. The Kuramoto model describes the all-to-all, uniformly coupled oscillators with purely sinusoidal interactions which can be solved analytically and provides a basic understanding of the mechanism of collective synchronization. Over the past few decades, the Kuramoto model has been recast in various forms to explore synchronization phenomena in different aspects, such as the effects of complex network topology [26–28], short-range interactions [29–32], time-delayed couplings [33–35], repulsive coupling [36,37], the presence of noises [38–40], various types of frequency distribution [41–45], etc. It is important to note that many of the above-mentioned problems can be solved analytically using a recent theoretical development by Ott and Antonsen; see Refs. [46,47] for more details.

It is of interest to explore the synchronization phenomenon of coupled oscillators with interactions decay over distance as a power law (i.e., interaction is proportional to $d^{-\alpha}$ where d is the distance between oscillators), since the interaction between biological oscillators diminishes as they are far apart. The nearest-neighbor coupling is a special case of the power-law coupling as $\alpha \to \infty$. Strogatz and Mirollo [30] and Daido [31] show independently that there is no long-range order in the thermodynamic limit for a one-dimensional chain. And in higher-dimensional lattices, spongelike clusters of synchronized oscillators are expected. For oscillators with long-range power-law interactions, Rogers and Wille [48] show through a numerical investigation for a one-dimensional system that as the range of interactions decreases a greater coupling strength is needed in order to achieve a synchronized state. However, synchronization cannot occur for finite coupling strength if $\alpha > 2$ [48]. Maródi *et al.* investigated a similar power-law coupling system but considered the realistic coupling that depends only on local phases and the distance between oscillators [49]. Their numerical results show that even if the coupling strength is arbitrarily weak, synchronization for large populations is possible if the power-law exponent is less than the dimensions of the lattice. Recently, Chowdhury and Cross presented analytical calculations and numerical simulations that demonstrate a transition from a synchronized state to an unsynchronized state for a sufficiently large but finite coupling strength when the power-law exponent is across 1.5 for oscillators on a one-dimensional lattice [50].

In this paper, we investigate the dynamical behavior of oscillators with long-range power-law interactions. We use a local order parameter that represents the degree of synchronization of individual oscillators to derive an analytical condition for synchronization. We show that if $\alpha \leqslant 1$ a system of locally coupled oscillators on a one-dimensional lattice is equivalent to a uniform coupling (all-to-all) system in the thermodynamic limit. For $\alpha > 1$, the system of oscillators could reach either a steady sync state or an oscillatory state, with finite coupling strength depending on the spatial distribution of the natural frequency. We use a coarse-graining method to analyze the oscillatory state. In particular, we analyze the two-plateau (two-cluster) system in detail and derive an analytical expression to predict breaking points of plateau splitting.

This paper is organized as follows: In Sec. II, we briefly review the Kuramoto model of locally coupled oscillators and introduce the local order parameter. With the local order parameter, we derive an analytical expression that is used to determine whether the locally coupled system would recover the analytical result for the all-to-all coupling system. In

*kuoan@phys.nthu.edu.tw

Sec. III, numerical investigation of critical coupling strength is discussed and a coarse-graining method is used to derive the criterion of plateau splitting. In Sec. IV, we analyze the characteristics of the oscillatory state in detail. In addition, the prediction of the breaking points of plateau splitting is made through the criterion of plateau splitting. Finally, the prediction of plateau splitting is examined by numerical simulations.

II. KURAMOTO MODEL OF LOCALLY COUPLED OSCILLATORS

A. Governing equations

The set of governing equations for the Kuramoto model of N locally coupled oscillators is ($i = 1, \ldots, N$)

$$\dot{\theta}_i = \omega_i + \frac{K}{\eta}\sum_{j=1}^{N} f(d_{ij})\sin(\theta_j - \theta_i), \tag{1}$$

where $\theta_{i,j}$ is the phase of i, jth oscillator, ω_i is the natural angular frequency chosen randomly from a symmetric distribution function $g(\omega)$, K is the coupling strength, $f(d_{ij})$ is the influence function that varies with the distance d_{ij} between the ith and jth oscillator, and η is a normalization constant defined as

$$\eta \equiv \sum_{j=1}^{N} f(d_{ij}). \tag{2}$$

For a positive influence function, the sinusoidal function ensures that the ith oscillator tends to catch up the phase of the jth oscillator. In this paper, we consider the oscillators are distributed in a one-dimensional chain and the periodic boundary condition is used. The natural frequency distribution function is chosen to have the form of the Lorentzian function with zero mean,

$$g(\omega) = \frac{\gamma}{\pi(\omega^2 + \gamma^2)}, \tag{3}$$

where γ is the half-width at half maximum. The influence function is set to be a monotonically decaying power-law function $f(d_{ij}) = d_{ij}^{-\alpha}$, where the exponent α determines the range of interaction ranging from the all-to-all coupling ($\alpha = 0$) to the nearest-neighbor coupling ($\alpha \to \infty$). For an all-to-all coupling system, the governing equations become

$$\dot{\theta}_i = \omega_i + \frac{K}{N}\sum_{j=1}^{N} \sin(\theta_j - \theta_i), \tag{4}$$

and the order parameter is defined as

$$Z = re^{i\phi} = \frac{1}{N}\sum_{j=1}^{N} e^{i\theta_j}, \tag{5}$$

where r is the amplitude of the order parameter Z representing the degree of synchronization of the system, and ϕ is the phase of the order parameter. The governing equation can be rewritten in a form that the ith oscillator is coupled to the mean field r and ϕ,

$$\dot{\theta}_i = \omega_i + Kr\sin(\phi - \theta_i). \tag{6}$$

The phase of the ith oscillator is coupled to the mean phase ϕ and with an effective coupling strength Kr. The oscillators can be divided into two groups: locked oscillators and drifting oscillators. From Eq. (6), the locked oscillators are those with the angular frequencies obeying $|\omega| \leqslant Kr$, and the drifting oscillators are those with the angular frequencies satisfying $|\omega| > Kr$. The system starts to synchronize as the coupling strength exceeds the critical coupling strength K_c, and right at the onset only oscillators with natural angular frequency around 0 are locked. Thus it is expected that the critical coupling strength depends on $g(0)$ but not the shape of $g(\omega)$. It is known that an all-to-all coupling system with the symmetric unimodal distribution function $g(\omega)$ starts to synchronize as the coupling strength K exceeds the critical coupling strength $K_c = 2/[\pi g(0)]$ and exhibits a supercritical bifurcation. For a Lorentzian distribution, the critical coupling strength is $K_c = 2\gamma$ and the degree of synchronization changes with K near the onset, $r = \sqrt{1 - K_c/K}$.

B. Local order parameter

For a locally coupled system, a local order parameter is defined in a similar way,

$$Z_j = \bar{r}_j e^{i\bar{\phi}_j} = \frac{1}{\eta}\sum_{\ell=1}^{N} f(d_{j\ell})e^{i\theta_\ell}. \tag{7}$$

Z_j is a locally weighted order parameter, and $\bar{r}_j$ and $\bar{\phi}_j$ represent the local degree of synchronization and its phase. Similarly, the governing equations of oscillators are coupled to the local order parameters,

$$\dot{\theta}_j = \omega_j + K\bar{r}_j\sin(\bar{\phi}_j - \theta_j). \tag{8}$$

The evolution of the phase for each oscillator depends on the local order parameter $\bar{r}_j$ and $\bar{\phi}_j$. Thus the dynamics of the locally coupled system is associated with the local order parameters and the variation of local order parameters. For simplicity, we assume N to be an odd number for the following derivation without loss of generality, and define $M = (N-1)/2$. In addition, the oscillators are spaced evenly and the distance between the adjacent oscillators is denoted by Δd. The variation of the local order parameter between two adjacent oscillators can be estimated by Eq. (7):

$$\begin{aligned} |Z_j - Z_{j+1}| &= |\bar{r}_j\, e^{i\bar{\phi}_j} - \bar{r}_{j+1}\, e^{i\bar{\phi}_{j+1}}| \\ &= \frac{1}{\eta}\left|\sum_{k=1}^{M} f(k\Delta d)\, e^{i\theta_{j+k}} + f(k\Delta d)\, e^{i\theta_{j-k}} - f(k\Delta d)\, e^{i\theta_{j+1+k}} - f(k\Delta d)\, e^{i\theta_{j+1-k}}\right| \end{aligned}$$

$$\approx \frac{1}{\eta}\left|\sum_{k=1}^{M-1}[f(k\Delta d)-f((k+1)\Delta d)]\,(e^{i\theta_{j-k}}-e^{i\theta_{j+k+1}})+f(\Delta d)\,(e^{i\theta_{j+1}}-e^{i\theta_j})\right|$$

$$\leqslant \frac{2}{\eta}\left(\sum_{k=1}^{M-1}[f(k\Delta d)-f((k+1)\Delta d)]+f(\Delta d)\right)\approx \frac{4f(\Delta d)}{\eta}\equiv\xi. \tag{9}$$

The maximum of the magnitude of the variation of the local order parameter between two adjacent oscillators is denoted by ξ, and it is proportional to the ratio of the influence function at the shortest distance $f(\Delta d)$ and is inversely proportional to the normalization constant η. In the case of $\xi \to 0$, the local order parameter is identical to the global order parameter, since $Z = (1/N)\sum_j Z_j = (1/N)\sum_j \bar{r}_j e^{i\bar{\phi}_j} = re^{i\phi}$. For locally coupled systems with $\xi \to 0$, the interaction of oscillators is long range so that the locally coupled systems behave the same way as the all-to-all coupling case. For a power-law influence function $f(d_{ij}) = d_{ij}^{-\alpha}$, ξ can be expressed as a ζ function in the limit $N \to \infty$:

$$\xi = 4\left(2\sum_{k=1}^{\infty}k^{-\alpha}\right)^{-1} = \frac{2}{\zeta(\alpha)}. \tag{10}$$

If one adopts the thermodynamic limit $N \to \infty$ and the long-range interaction $0 \leqslant \alpha \leqslant 1$, the local variation ξ becomes zero, since $\zeta(\alpha)$ diverges and the locally coupled system is equivalent to the all-to-all coupling case. And the value of the critical coupling strength starts to deviate from that in the global case, as α is greater than unity. The critical exponent $\alpha_c = 1$ agrees with earlier studies of power-law coupling systems [48–50]. Figure 1 plots numerical results for the degree of synchronization against the coupling strength for $\alpha \leqslant 1$ and $\alpha > 1$. Numerically, the degree of synchronization is the time-averaged value of r after the transient period. The simulations are carried out using Eq. (1) with 1,024 oscillators for $\alpha \leqslant 1$ and 10,112 oscillators for $\alpha > 1$, and the half-width at half maximum of the Lorentzian distribution $\gamma = 0.4$. Note that γ is set to be 0.4 for all numerical simulations presented in this paper. The corresponding critical coupling strength for the all-to-all coupling case in the thermodynamic limit is $K_c = 2\gamma = 0.8$. The bifurcation curves for $\alpha \leqslant 1$ are in quantitative agreement with the bifurcation curve for the all-to-all coupling case [see Fig. 1(a)], while the bifurcation curves shift toward a higher coupling strength for $\alpha > 1$ [see Fig. 1(b)]. Thus one can determine whether the locally coupled systems follow the prediction of the globally coupled systems by testing the convergence of the variation of the local order parameters.

III. STATIONARY SYNCHRONIZATION AND OSCILLATORY STATES

A. Bistability

For coupled oscillators with a power-law interaction and the power-law exponent $\alpha > 1$, the outcome of the degree of synchronization as $t \to \infty$ is determined by the spatial distribution of the natural angular frequency of oscillators. The degree of synchronization of coupled oscillators r either reaches a stationary value, which signals that all locked oscillators are in sync, or becomes oscillatory over time, which indicates that more than one locally synchronized cluster of oscillators is formed. We define the probability $P(K)$ as the probability of locally coupled systems reaching the nonzero stationary synchronization for a given coupling strength K. For $\alpha \leqslant 1$, in the thermodynamic limit, the probability function $P(K)$ is simply a step function that $P(K)$ jumps from 0 to 1 as the coupling strength exceeds K_c. Numerically, we investigate the probability function $P(K)$ for $\alpha > 1$ using $N = 10{,}112$ and $\gamma = 0.4$. The probability function $P(K)$ calculated from 100 independent simulations against α is plotted in Fig. 2. For

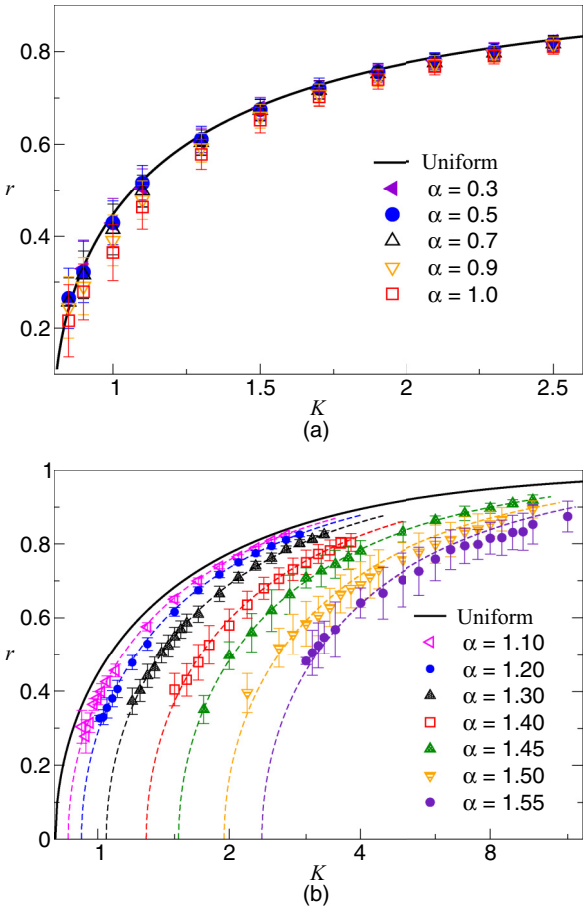

FIG. 1. (Color online) The degree of synchronization r against the coupling strength K is plotted in (a) and (b) for $\alpha \leqslant 1$ and $\alpha > 1$, respectively. Results of numerical simulations are plotted in symbols and are compared to the theoretical prediction of the uniform coupling system (black line). Note that the K axis is plotted in linear and logarithmic scale in (a) and (b), respectively. And the number of oscillators used in simulations is 1,024 and 10,112 in (a) and (b), respectively.

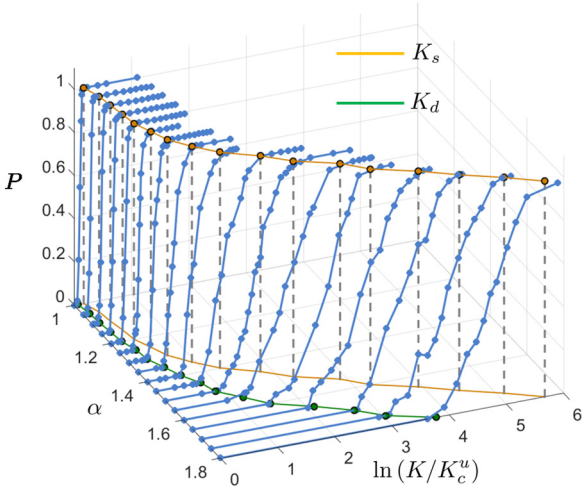

FIG. 2. (Color online) Probability of locally coupled systems from numerical simulations reaching a nonzero stationary sync state as a function of power-law exponent α and coupling strength K. The locally coupled systems could reach stationary sync states once the coupling strength is greater than K_d. And the systems always reach stationary sync states as $K > K_s$. Note that K_c^u denotes the theoretical critical coupling strength for the uniform coupling system.

$\alpha > 1$, the probability function is a smooth function remaining at 0 if the coupling strength is less than K_d. Once the coupling strength exceeds K_d, the probability function rises smoothly and eventually reaches unity at K_s. The K_s and K_d curves against α suggest that both values grow exponentially with α for $\alpha > 1.5$ (see Fig. 3).

B. Oscillatory state and plateau splitting

A plateau or a cluster is a domain of oscillators in which locked oscillators have the same time-averaged angular frequency. The time-averaged angular frequency of i oscillators

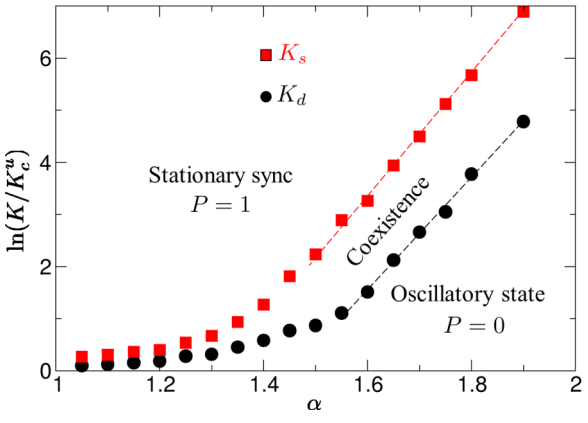

FIG. 3. (Color online) The phase diagram of stationary sync states, oscillatory states, and the coexistence region is obtained from numerical simulations (see Fig. 2). The oscillatory states appear as $K < K_d$, and the probability of obtaining the oscillatory state diminishes as K approaches K_s. For $\alpha > 1.5$, both K_s and K_d curves are best fitted by straight lines (dashed lines). Note that K_c^u denotes the theoretical critical coupling strength for the uniform coupling system.

is defined as

$$\tilde{\omega}_i(t) = \frac{\theta_i(t+T_o) - \theta_i(t-T_o)}{2T_o}, \tag{11}$$

where T_o is taken to be a period of time that is much larger than $2\pi/\omega_i$. The relative phase difference of locked oscillators in a plateau must remain the same, since within a plateau phases of oscillators are rotating with the same time-averaged angular frequency. The stationary synchronization is a result of coherent movement of all locked oscillators, which indicates a single macroscopic plateau. Rogers and Wille have reported that a macroscopic plateau splits into two or more plateaus as K decreases or α increases [48]. As multiple plateaus form, one starts to observe the oscillatory state of r due to incoherent motion between plateaus. Therefore, it is of interest to predict at which value of K and α the single plateau would split into two plateaus, and at which oscillators the plateau splits. We discuss the criterion of plateau splitting in this section and use this criterion to predict the breaking points of the plateau in Sec. IV. In the following, we investigate the onset of plateau splitting: the two-plateau state.

We assume that two plateaus, namely, A and B, are presented in a one-dimensional ring, and the number of oscillators in plateau A and B is N_A and N_B, respectively. The governing equations for oscillators in each plateau are

$$\begin{aligned} \dot{\theta}_i &= \omega_i + \frac{K}{\eta}\sum_{j\neq i} f(d_{ij})\sin(\theta_j - \theta_i) \qquad i \in \{A\}, \\ \dot{\theta}_i &= \omega_i + \frac{K}{\eta}\sum_{j\neq i} f(d_{ij})\sin(\theta_j - \theta_i) \qquad i \in \{B\}. \end{aligned} \tag{12}$$

The mean angular velocity of each plateau is obtained by taking the average over all oscillators within the same plateau. We obtain

$$\begin{aligned} \langle\dot{\theta}_A\rangle &= \langle\omega_A\rangle + \frac{K}{N_A}\sum_{i\in A}\sum_{j\in B}\frac{f(d_{ij})}{\eta}\sin(\theta_j - \theta_i), \\ \langle\dot{\theta}_B\rangle &= \langle\omega_B\rangle + \frac{K}{N_B}\sum_{i\in B}\sum_{j\in A}\frac{f(d_{ij})}{\eta}\sin(\theta_j - \theta_i), \end{aligned} \tag{13}$$

where $\langle\cdots\rangle$ denotes averaging over oscillators within a plateau. The interaction terms involved with oscillators within the same plateau cancel out each other due to asymmetry of the sinusoidal coupling function. By the above coarse-grained approach, the locally coupled system can be seen as a two-oscillator system. Each coarse-grained oscillator has a natural angular frequency that is the average of the natural angular frequencies of oscillators within the plateau. And the coupling between these two coarse-grained oscillators is merely related to the sum of all cross-plateau pair interactions. By defining an effective coupling function,

$$\chi \equiv \sum_{i\in A}\sum_{j\in B}\frac{f(d_{ij})}{\eta}\sin(\theta_j - \theta_i), \tag{14}$$

the difference between the mean angular velocity of plateau A and B can be written as

$$\langle\dot{\theta}_A\rangle - \langle\dot{\theta}_B\rangle = \langle\omega_A\rangle - \langle\omega_B\rangle + K\chi\left(\frac{1}{N_A} + \frac{1}{N_B}\right). \tag{15}$$

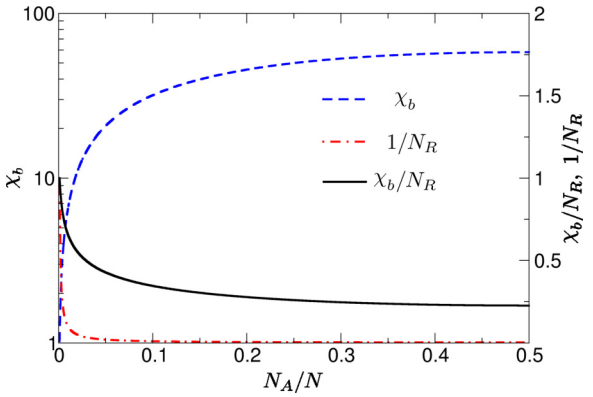

FIG. 4. (Color online) The criterion of plateau splitting is given by Eq. (16), which is inversely proportional to χ_b/N_R. We plot χ_b/N_R as a function of number fraction of oscillators in plateau A for $\alpha = 1.1$ and $N = 1{,}024$.

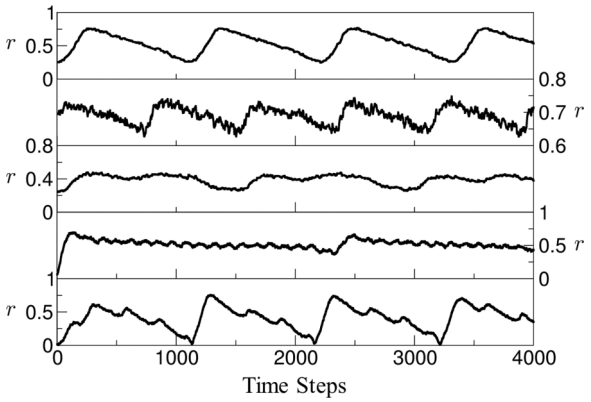

FIG. 5. Examples from numerical simulations of oscillatory states for power-law coupled systems with parameters $\alpha = 1.4$, $N = 1{,}024$, and $K = 2.0$ for the bottom two figures and $K = 2.5$ for the top three figures. The time step used in simulations is $dt = 1/8$ and $dt = 1/40$ for $K = 2.0$ and $K = 2.5$, respectively.

The plateau splitting vanishes as the left-hand side of Eq. (15) equals zero. For a power-law influence function, the value of the effective coupling function is bounded, $-\chi_b < \chi < \chi_b$, where $\chi_b = \sum_{i\in A}\sum_{j\in B} f(d_{ij})/\eta$, since $f(d_{ij})$ is always greater than zero. Thus we define p to be the ratio of the natural angular frequency difference and the effective coupling strength between two plateaus,

$$p \equiv \frac{|\langle\omega_A\rangle - \langle\omega_B\rangle|}{K\chi_b/N_R}, \tag{16}$$

where $1/N_R \equiv 1/N_A + 1/N_B$. For $p \geqslant 1$, the difference in mean natural angular frequency between plateaus A and B overcomes the attractive interaction so that the system forms two plateaus. Equation (16) gives a quantitative relation of the formation of two plateaus for a given set of parameters. It is clear that as the coupling strength K decreases or α increases the value of p increases. Furthermore, χ_b increases as the fraction of plateau A increases and reaches its maximum when two plateaus have an equal number of oscillators (i.e., $N_A/N = 0.5$). In contrast, $1/N_R$ is a monotonically decreasing function as the fraction of plateau A increases from 0 to 0.5. The product of χ_b and $1/N_R$ as a function of the fraction of plateau A is plotted in Fig. 4 for $\alpha = 1.1$ and $N = 1{,}024$. The value of χ_b/N_R reaches its minimum at $N_A/N = 0.5$, which suggests that the maximum value of p occurs as two plateaus have the same size. Nevertheless, the value of p also depends on the difference between the mean natural angular frequency of plateaus. Thus the spatial distribution of the natural frequency of oscillators is the main determinant of plateau splitting. Therefore, the locally coupled oscillators could either reach a stationary sync state or an oscillatory state that completely relies on the initial spatial distribution of the natural frequency; see the coexistence region in Fig. 3. With a given spatial distribution of the natural frequency, Eq. (16) can be used to predict the breaking points of plateaus as discussed in the following section.

IV. OSCILLATORY STATE ANALYSIS

The oscillatory behavior of the global order parameter $r(t)$ is a result of the dynamics of unsynchronized coarse-grained oscillators as discussed in the previous section. The oscillatory state becomes more complex as more plateaus are formed in the system. Various oscillatory behaviors of $r(t)$ are illustrated in Fig. 5 for $\alpha = 1{,}4$, $N = 1{,}024$, and various coupling strengths K. The mechanism for the oscillatory behavior is intuitive. When the mean phase of any two clusters of oscillators approaches each other, the global order parameter $r(t)$ increases accordingly. On the contrary, $r(t)$ decreases as the mean phase of plateaus runs away from each other. Thus the phase coherence $r(t)$ rises and falls periodically.

A. Characteristics of the two-plateau state

The behavior of two-plateau oscillatory state can be quantified by its amplitude and period. The amplitude of $r(t)$ is defined as the difference of its maximum and minimum values. The maximum of $r(t)$ occurs when two plateaus reach the same mean phase, $\langle\theta_A\rangle = \langle\theta_B\rangle$, while the minimum occurs when two plateaus are out of phase, $\langle\theta_A\rangle = -\langle\theta_B\rangle$. For simplicity, we take the smaller plateau to be plateau A in the following discussion. The amplitude of $r(t)$ is obtained straightforwardly $r_{\max} - r_{\min} = 2r_A N_A/N$, where r_A is the degree of synchronization of plateau A. The amplitude is proportional to the size of the smaller plateau. Simulations of locally coupled systems are carried out with different values of α and K, and Fig. 6 shows a linear relation between the amplitude and N_A/N for 67 two-plateau states. On the other hand, the frequency of the oscillatory state derived from the two-plateau state is linearly proportional to the difference of the mean angular velocity of two plateaus that is consistent with results of numerical simulations.

B. Prediction of breaking points of plateau splitting

Equation (16) can be used to predict the breaking points of the two-plateau state. For the above-mentioned locally coupled system, the nearest-neighbor coupling is the strongest and plays a crucial role in influencing the phases of oscillators nearby. The nearest-neighbor coupling becomes effectively weak around drifting oscillators, since the phase of drifting oscillators drifts and the time average coupling is negligible. Therefore, for a single plateau system, as the coupling strength

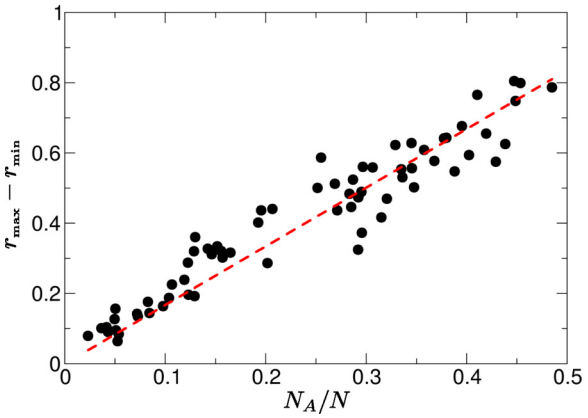

FIG. 6. (Color online) The amplitude of the oscillatory state $r(t)$ against the size fraction of a smaller plateau for a two-plateau state. The numerical results (solid circles) are obtained from 67 oscillatory states and can be fitted linearly as predicted by the theory (dashed line).

K decreases one would expect the single plateau to split into two plateaus around a certain pair of drifting oscillators. In order to predict the breaking points, we first identify locations of drifting oscillators by the relation $|\omega_i| > Kr$, where r is the degree of synchronization of the single plateau state right before plateau splitting. With the locations of drifting oscillators, we calculate the value of p using Eq. (16) for all possible pairs of breaking points. The value of p for different pairs of breaking points is plotted in Fig. 7(a) for 1,024 oscillators, $\alpha = 1.4$, $K = 2.5$; two pairs of breaking points with large value of p are found around (6,311) and (311,1012). The corresponding simulation results show that breaking points occur at (6,311) [see Fig. 7(b)]. The value of p calculated using Eq. (16) must be greater than unity for plateau splitting. However, it is found numerically that plateau splitting occurs when p is less than unity in some cases, because previously we used the upper bound value of coupling terms to estimate p. In order to give a more accurate prediction of breaking points, we furthermore consider the details of phase dispersion of locked oscillators in the following section.

C. Phase dispersion

For locked oscillators in a plateau, Eq. (8) gives the relation between the phase of the oscillator and its natural frequency,

$$\theta_i = \bar{\phi}_i + \arcsin\left(\frac{\omega_i}{K\bar{r}_i}\right). \tag{17}$$

At the onset of plateau splitting, $\bar{r}_i$ can be approximated by the degree of synchronization r right before plateau splitting. The simulation results are in quantitatively good agreement with Eq. (17) (see Fig. 8). In addition, $\bar{\phi}_i$ can be well approximated by the mean phase of the plateau. Therefore, in the two-plateau system, the phase of a locked oscillator in plateau A or B is approximately

$$\begin{aligned} \theta_i &= \langle\theta_A\rangle + \arcsin\left(\frac{\omega_i}{Kr}\right) \quad i \in A, \\ \theta_i &= \langle\theta_B\rangle + \arcsin\left(\frac{\omega_i}{Kr}\right) \quad i \in B. \end{aligned} \tag{18}$$

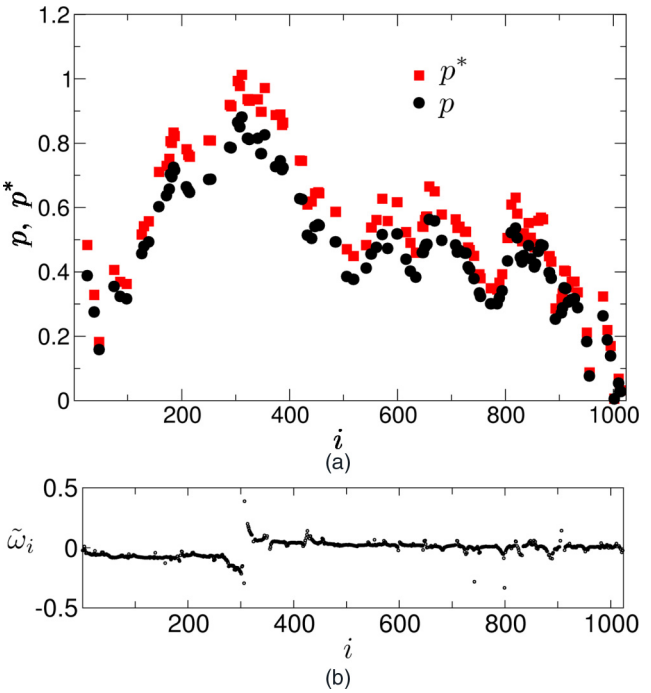

FIG. 7. (Color online) (a) For a given frequency distribution, the value of p calculated from Eq. (16) (circles) and the value of p^* from Eq. (20) (squares) as functions of the position of the breaking point. (The other breaking point is set to be located at $i = 6$.) The maximum values of p and p^* occur around the pair of breaking points (6,311). (b) A snapshot of time-averaged angular frequency from the simulation that illustrates the plateau splits around the oscillator pair (6,311). Parameters used in simulations are $\alpha = 1.4, N = 1{,}024$, and $K = 2.5$.

The phases of locked oscillators with $\omega > 0$ are ahead of the mean phase of the plateau, while the phases of locked oscillators with $\omega < 0$ are behind of the mean phase of

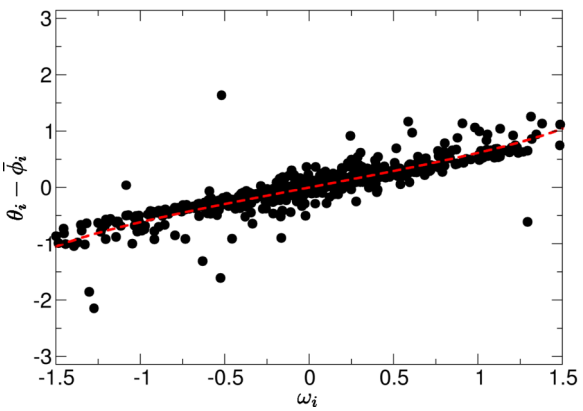

FIG. 8. (Color online) The difference between the phase of the oscillator and the phase of the local order parameter against its natural angular frequency from numerical simulations (circles). The phase dispersion distribution is in quantitative agreement with Eq. (17), $\theta_i - \bar{\phi}_i = \arcsin[\omega_i/(Kr)]$, where $K = 2.5$ and $r = 0.69$ (dashed line). The value of r employed here is the degree of synchronization just right before the onset of plateau splitting. The simulation parameters are $\alpha = 1.4$ and $N = 1{,}024$.

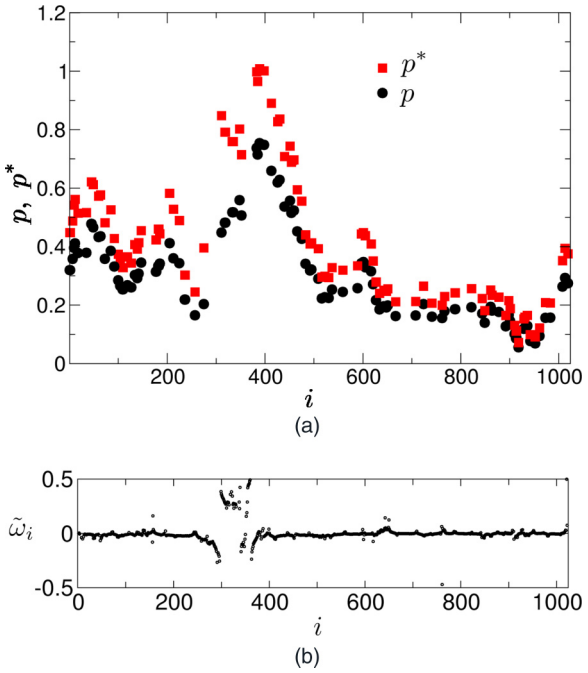

FIG. 9. (Color online) (a) For a given frequency distribution, the value of p calculated from Eq. (16) (circles) and the value of p^* from Eq. (20) (squares) as functions of the position of the breaking point. (The other breaking point is set to be located at $i = 293$.) The maximum values of p and p^* occur around the pair of breaking points (293,389). (b) A snapshot of time-averaged angular frequency from the simulations that illustrates the plateau splits around the oscillator pair (293,389). Parameters used in simulations are $\alpha = 1.4, N = 1{,}024$, and $K = 2.5$.

the plateau. Since the coupling between two plateaus is the strongest when the phase difference between two plateaus is $\pi/2$, we consider the special case where $\langle\theta_A\rangle - \langle\theta_B\rangle = \pi/2$. By taking into account the dispersion of phases, the effective coupling term becomes a bit smaller,

$$\begin{aligned}\chi &= \sum_{i\in A}\sum_{j\in B}\frac{f(d_{ij})}{\eta}\sin(\theta_j-\theta_i)\\ &= \sum_{i\in A}\sum_{j\in B}\frac{f(d_{ij})}{\eta}\left[\sqrt{1-\left(\frac{\omega_j}{Kr}\right)^2}\sqrt{1-\left(\frac{\omega_i}{Kr}\right)^2}+\frac{\omega_j}{Kr}\frac{\omega_i}{Kr}\right]\\ &\approx \sum_{i\in A}\sum_{j\in B}\frac{f(d_{ij})}{\eta}\left[1-\frac{1}{2}\left(\frac{\omega_j-\omega_i}{Kr}\right)^2\right],\end{aligned} \tag{19}$$

which gives rise to a more accurate criterion for plateau splitting,

$$p^* = \frac{N_R\eta}{K}\cdot\frac{|\langle\omega_A\rangle-\langle\omega_B\rangle|}{\sum_{i\in A}\sum_{j\in B}f(d_{ij})[1-(\omega_j-\omega_i)^2/(\sqrt{2}Kr)^2]}. \tag{20}$$

Numerically, Eq. (20) gives a more accurate prediction of the breaking points. One more example is shown in Fig. 9 where both Eqs. (16) and (20) predict that the pair of the breaking points occurs around (293,389). Nevertheless, the value of p calculated using Eq. (16) is less than unity, while it is greater than unity calculated using Eq. (20).

V. CONCLUSION

We investigate the synchronization phenomena for locally coupled oscillators located on a one-dimensional ring. In particular, we employ oscillators with a power-law interaction, $d^{-\alpha}$. One recovers a uniform coupling system as $\alpha \to 0$, and a nearest-neighbor coupling system as $\alpha \to \infty$. We introduce a local order parameter that represents the degree of local synchronization, and the individual oscillator can be seen to couple to the local order parameter. Using the local order parameter, we define the maximum variation of the magnitude of the local order parameter ξ. In the thermodynamic limit, ξ is inversely proportional to the ζ function, which becomes zero for $\alpha \leqslant 1$. Thus in the limit of $N \to \infty$, the locally coupled systems with $\alpha \leqslant 1$ are equivalent to the uniform all-to-all system. Similarly, one can determine whether a group of oscillators with an arbitrary form of interaction can be reduced to an all-to-all coupling system by examining if the parameter ξ vanishes or not. If ξ does not vanish, the difference between the local order parameter propagates through the one-dimensional chain, and the system could reach either a stationary synchronized state or an oscillatory state, depending on the initial spatial arrangement of the natural angular frequency. For the oscillatory state, the phase coherence changes periodically over time. The oscillatory nature is due to the splitting of oscillators into multiple groups, which can be analyzed by treating groups of oscillators as coarse-grained oscillators.

We analyze the simplest oscillatory state, namely, the two-plateau system. By considering the two-plateau system as two coarse-grained oscillators, we derive an expression for the criterion of plateau splitting [see Eq. (16)]. The value of p is intuitively proportional to the difference of the natural angular frequency of coarse-grained oscillators and is inversely proportional to the coupling strength and the effective coupling function. In addition, the value of p also depends on the ratio of the size of two plateaus. With a given spatial distribution of the natural angular frequency, one is able to predict breaking points of plateau splitting accordingly. Furthermore, a more accurate prediction of breaking points can be made by considering the details of phase dispersion of individual oscillators. However, as the number of oscillators increases, the assumption that the local order parameter of oscillators in a single plateau is approximately the same is no longer valid, since the local order parameter could vary slowly over space. Furthermore, numerical results show that the boundary between two plateaus is rather fuzzy and not sharp. Thus a more refined approach to predict the breaking points should take into account these effects. Nevertheless, the expression of the criterion of plateau splitting is still valid for a finite network of oscillators and provides a qualitative way to estimate when and where the plateau splits.

ACKNOWLEDGMENTS

We gratefully acknowledge the support of the National Science Council of Taiwan (NSC102-2112-M-007-007-MY3), and we acknowledge the support of National Center for Theoretical Sciences, Taiwan.

[1] J. C. Neu, SIAM J. Appl. Math. **38**, 305 (1980).
[2] Y. Kuramoto, *Chemical Oscillations, Waves and Turbulence* (Springer, Berlin, 1984).
[3] M. S. Paoletti, C. R. Nugent, and T. H. Solomon, Phys. Rev. Lett. **96**, 124101 (2006).
[4] P. Hadley, M. R. Beasley, and K. Wiesenfeld, Phys. Rev. B **38**, 8712 (1988).
[5] K. Wiesenfeld, P. Colet, and S. H. Strogatz, Phys. Rev. E **57**, 1563 (1998).
[6] P. Hadley, M. R. Beasley, and K. Wiesenfeld, Am. J. Phys. **70**, 10 (2002).
[7] G. Filatrella, N. F. Pedersen, and K. Wiesenfeld, Phys. Rev. E **75**, 017201 (2007).
[8] Z. Néda, E. Ravasz, T. Vicsek, Y. Brechet, and A. L. Barabási, Phys. Rev. E **61**, 6987 (2000).
[9] Z. Néda, E. Ravasz, Y. Brechet, T. Vicsek, and A. L. Barabasi, Nature (London) **403**, 849 (2000).
[10] M. Bennett, M. F. Schatz, H. Rockwood, and K. Wiesenfeld, Proc. R. Soc. London, Sect. A **458**, 563 (2002).
[11] J. Pantaleone, Am. J. Phys. **70**, 992 (2002).
[12] S. H. Strogatz, D. M. Abrams, A. McRobie, B. Eckhardt, and E. Ott, Nature (London) **438**, 43 (2005).
[13] J. Buck and E. Buck, Science **159**, 1319 (1968).
[14] J. Buck and E. Buck, Sci. Am. **234**, 74 (1976).
[15] J. Buck, Quart. Rev. Biol. **63**, 265 (1988).
[16] M. G. Kitzbichler, M. L. Smith, S. R. Christensen, and E. Bullmore, PLoS Comput. Biol. **5**, e1000314 (2009).
[17] R. E. Mirollo and S. H. Strogatz, SIAM J. Appl. Math. **50**, 1645 (1990).
[18] S. H. Strogatz and I. Stewart, Sci. Am. **269**, 102 (1993).
[19] C. M. Gray, J. Comput. Neurosci. **1**, 11 (1994).
[20] H. Ando, H. Suetani, J. Kurths, and K. Aihara, Phys. Rev. E **86**, 016205 (2012).
[21] M. Botcharova, S. F. Farmer, and L. Berthouze, Phys. Rev. E **86**, 051920 (2012).
[22] A. T. Winfree, J. Theor. Biol. **16**, 15 (1967).
[23] Y. Kuramoto, *International Symposium on Mathematical Problems in Theoretical Physics*, edited by H. Araki, Lecture Notes in Physics Vol. 39 (Springer, Berlin, 1975), p. 420.
[24] S. H. Strogatz, Physica D **143**, 1 (2000).
[25] J. A. Acebrón, L. L. Bonilla, C. J. Pérez Vicente, F. Ritort, and R. Spigler, Rev. Mod. Phys. **77**, 137 (2005).
[26] S. H. Strogatz, Nature (London) **410**, 268 (2001).
[27] A. Arenas, A. Díaz-Guilera, and C. J. Pérez-Vicente, Phys. Rev. Lett. **96**, 114102 (2006).
[28] A. Arenas, A. Díaz-Guilera, J. Kurths, Y. Moreno, and C. Zhou, Phys. Rep. **469**, 93 (2008).
[29] H. Sakaguchi, S. Shinomoto, and Y. Kuramoto, Progr. Theor. Phys. **77**, 1005 (1987).
[30] S. H. Strogatz and R. E. Mirollo, J. Phys. A **21**, L699 (1988).
[31] H. Daido, Phys. Rev. Lett. **61**, 231 (1988).
[32] S. H. Strogatz and R. E. Mirollo, Physica D **31**, 143 (1988).
[33] D. V. Ramana Reddy, A. Sen, and G. L. Johnston, Phys. Rev. Lett. **80**, 5109 (1998).
[34] M. K. S. Yeung and S. H. Strogatz, Phys. Rev. Lett. **82**, 648 (1999).
[35] C. Li and G. Chen, Phys. A (Amsterdam, Neth.) **343**, 263 (2004).
[36] L. S. Tsimring, N. F. Rulkov, M. L. Larsen, and M. Gabbay, Phys. Rev. Lett. **95**, 014101 (2005).
[37] H. Hong and S. H. Strogatz, Phys. Rev. Lett. **106**, 054102 (2011).
[38] H. Sakaguchi, Progr. Theor. Phys. **79**, 39 (1988).
[39] Y. Kuramoto, Physica D **50**, 15 (1991).
[40] J.-n. Teramae and D. Tanaka, Phys. Rev. Lett. **93**, 204103 (2004).
[41] S. H. Strogatz and R. E. Mirollo, J. Stat. Phys. **63**, 613 (1991).
[42] J. A. Acebrón and R. Spigler, Phys. Rev. Lett. **81**, 2229 (1998).
[43] J. A. Acebrón, L. L. Bonilla, and R. Spigler, Phys. Rev. E **62**, 3437 (2000).
[44] E. A. Martens, E. Barreto, S. H. Strogatz, E. Ott, P. So, and T. M. Antonsen, Phys. Rev. E **79**, 026204 (2009).
[45] D. Pazó and E. Montbrió, Phys. Rev. E **80**, 046215 (2009).
[46] E. Ott and T. M. Antonsen, Chaos **18**, 037113 (2008).
[47] E. Ott and T. M. Antonsen, Chaos **19**, 023117 (2009).
[48] J. L. Rogers and L. T. Wille, Phys. Rev. E **54**, R2193 (1996).
[49] M. Maródi, F. d'Ovidio, and T. Vicsek, Phys. Rev. E **66**, 011109 (2002).
[50] D. Chowdhury and M. C. Cross, Phys. Rev. E **82**, 016205 (2010).